Central European Journal of Energetic Materials
ISSN 1733-7178; e-ISSN 2353-1843

Cent. Eur. J. Energ. Mater. 2024, *21*(2): 138-152; DOI 10.22211/cejem/190415
Article is available in PDF-format, in colour, at:
https://ipo.lukasiewicz.gov.pl/wydawnictwa/cejem-woluminy/vol-21-nr-2/

Research paper

Study of the Progress of Reaction in the Preparation of tetra-Functional GAP using FTIR Spectroscopy

Prasanta Kumar Adak[1,*], **Ashish Kumar Meena**[1], **Mrinal Ghosh**[1], **Vikas Sutar**[1], **Mukesh Jain**[1], **Shaibal Banerjee**[2]

[1] *High Energy Materials Research Laboratory, Sutarwadi, Pune-411 021, India*

[2] *Defence Institute of Advanced Technology, Girinagar, Pune-411 025, India*

* *E-mail:* adak.pk.hemrl@gov.in

Abstract: Glycidyl azide polymer (GAP) with tetra hydroxyl functional groups or t-GAP is a potential energetic polymeric binder for application in both high energy propellants and high explosives. t-GAP is synthesized via azidation of the precursor tetrafunctional poly-epichlorohydrine (t-PECH) with sodium azide in DMSO solvent medium. In this article, process optimization and progress of chemical reaction for preparation of t-GAP is studied using FTIR spectroscopy and an attempt is made to predict the reaction kinetics with concentration profiling. The characteristic vibrational features corresponding to C–N_3 of t-GAP and C–Cl of t-PECH have been used to monitor the progress of reaction.

Keywords: energetic binder, FTIR, reaction kinetics, reaction profiling, t-GAP

1 Introduction

The development of energetic binders has always been a key research area in the development of both high energy propellants for application in rockets/

missiles and high explosive formulations for application in warheads. Glycidyl azide polymer (GAP) with two or more hydroxyl groups is one such energetic binder [1-6]. GAP is widely used as an energetic binder along with ammonium dinitramide (ADN) as a green and chlorine free oxidizer in high energy composite propellants and gas generating compositions [7-13]. Klapotke *et al.* [14] have reported GAP/TKX-50 based rocket propellant formulations. GAP also finds application in plastic bonded explosives as an energetic binder in place of conventional inert binders like hydroxyl terminated polybutadiene (HTPB) [15].

GAP based energetic binders possess positive heat of formation, higher density and excellent thermal stability. It offers a significantly higher specific impulse and superior ballistic properties compared to conventional binders like HTPB and carboxy terminated polybutadiene (CTPB) etc. The di-functional GAP (d-GAP) with two terminal hydroxyl groups imparts a higher specific impulse along with ADN in the propellant, both with and without aluminium. However, it exhibits poor mechanical properties compared to HTPB based propellants. In addition, the hydroxyl groups in d-GAP are secondary in nature and therefore curing with di-isocyanates needs to be carried out at a relatively higher temperature. In order to improve the characteristics of GAP, synthesis of tetra hydroxyl functional GAP or GAP tetraol (t-GAP) with both primary and secondary terminal hydroxyl groups has been developed. t-GAP was first prepared in 1994 through the azidation of tetra hydroxyl polyepichlorohydrin (t-PECH) which was obtained by the epoxidation of PECH diol, followed acid hydrolysis [16]. Recently, Soman et al. [17] reported a method for preparing t-GAP, rheological characterization during its curing and evaluation of its mechanical properties. In both methods, t-PECH had been subjected to azidation with sodium azide (NaN_3), in an aprotic polar solvent like DMF or DMSO. The polymeric and energetic properties of t-GAP are well reported. However, there is no data available in literature on the reaction kinetics of the azidation process for t-GAP. In this study, the process for t-GAP was studied on a laboratory scale. Based on laboratory scale experiments, the process has been optimized with respect to temperature and time. FTIR spectrometry is an established tool and has been widely used to study the progress of various types of reaction and to derive their kinetic data [18, 19]. The same has been used to derive the kinetic data and rate equation for the t-GAP process.

The reaction progress of a bench scale batch (at 0.5 kg level) of t-GAP has been periodically tested using FTIR spectroscopy to find the reaction end point and to obtain kinetic parameters. t-GAP is synthesized via azidation of the precursor t-PECH with NaN_3 in DMSO as the reaction medium (Figure 1). The reaction of NaN_3 and t-PECH passes through the nucleophilic substitution of –Cl

by $-N_3$. The characteristic vibrational features corresponding to C–N_3 of t-GAP and C–Cl of t-PECH have been employed to derive the progress of the reaction.

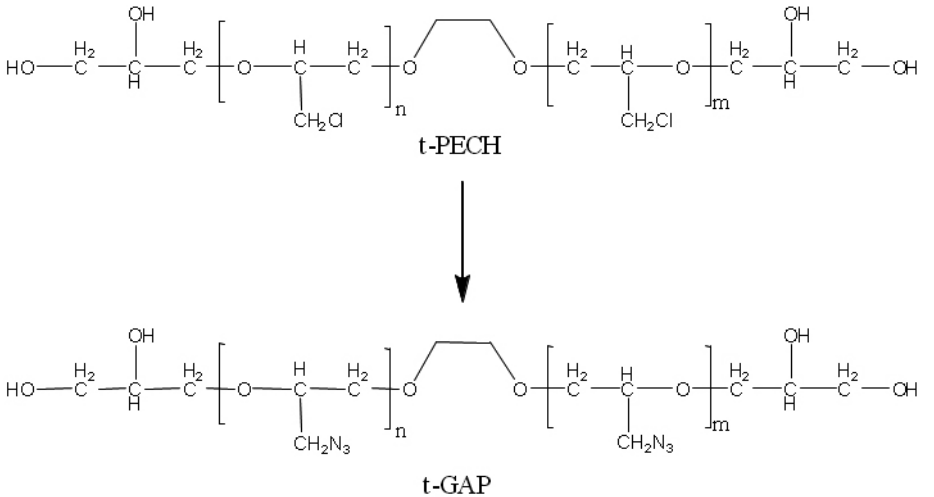

Figure 1. Azidation of t-PECH for preparation of t-GAP

The area under the curve of respective IR vibrational peaks of t-GAP and t-PECH has been considered to be a direct representation of their concentration in the reaction mixture. The real time profiling has thus been useful in earmarking the actual time required for complete azidation of t-PECH to t-GAP. The concentration profile has further been employed to calculate the kinetic parameters such as order of reaction (n) and rate constant using both integral and differential methods of rate kinetics [13].

2 Experimental

2.1 Materials

The precursor material, t-PECH was obtained from a commercial source with the properties:

- molecular weight (M_n): 1500 ±50,
- hydroxyl/OH value: 87 ±2 mg KOH/g,
- viscosity: 52 ±5 P,
- volatile matter (VM): 0.01-0.03%, and
- moisture content 0.03-0.06%.

Other chemicals and reagents like NaN_3, DMSO and ethyl acetate used in the process were of GR grade (purity >95%) and were obtained from Qualigen and Merck.

2.2 Experimental set-up for t-GAP synthesis

The bench scale process for t-GAP was carried out in a bench scale reactor set-up (*HEL, UK make)*. The chemical reaction was performed in a 10 L jacketed reactor fitted with a double coiled reflux condenser. Heating and cooling of the reaction mixture was ensured with a highly efficient Huber circulator system. Reaction parameters like *T*r, *T*j, Δ*T*, RPM *etc*. were controlled and recorded through an attached PLC-SCADA system. A 50 L volume glass reactor fitted with overhead stirrer was used for extraction of t-GAP.

2.3 Preparation of t-GAP

A slurry of NaN_3 in DMSO is prepared in a 10 L reactor at around 40-45 °C under constant agitation. The slurry was then slowly heated up to the reaction temperature followed by the dropwise addition of a solution of t-PECH in DMSO. Care was taken during addition of t-PECH solution to avoid an uncontrolled rise in temperature. The reaction mixture turned light brown towards the end of addition. During the process, samples were withdrawn periodically at distinct time intervals and analyzed using FTIR spectroscopy to monitor the progress of the reaction. At the end of the reaction, the reaction mass was cooled to 60 °C and then quenched in a volume of 50 L fed with ice-water mixture. It was observed that the reaction mass became very thick at a temperature below 55 °C, thus, the reaction mass was taken out of the reactor at about 60 °C.

(a) (b) (c)

Figure 2. Various stages of t-GAP process: final reaction mass (a), mass during quenching (b) and t-GAP (c)

A suitable solvent was then added to the reaction mass in the quencher and stirred for 2-3 h and was subsequently washed with 10% NaCl solution. The organic phase was separated and the solvent distilled off under vacuum.

2.4 Spectral analysis

A table top FTIR spectrometer (Thermo Fisher Scientific Nicolet Summit pro) was used to record the IR absorption data of the reaction mixture samples. The sample collected from the reaction mass was directly analyzed using single bounce Diamond ATR accessory. t-PECH was characterized by a medium to strong IR absorption peak at 747 cm^{-1} corresponding to C–Cl stretching vibration while, t-GAP was characterized by a strong peak at 2088 cm^{-1} corresponding to $–N_3$ stretching vibration. A comparative FTIR profile is presented in Figure 3. IR Spectrums were recorded for the samples withdrawn periodically at 1 h intervals.

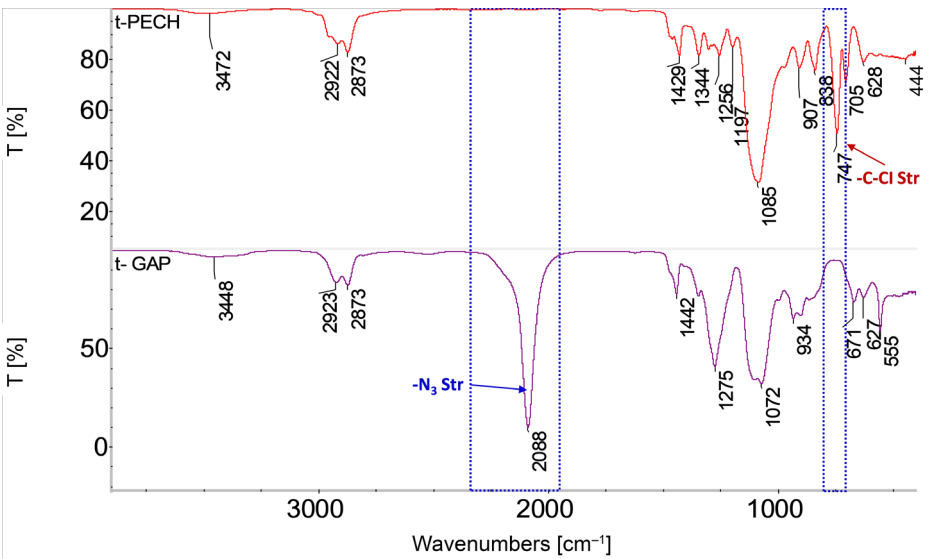

Figure 3. Comparative FTIR spectral data of t-PECH and t-GAP

2.5 Characterization

The physical and chemical properties of t-GAP were determined using various instrumental techniques. Average molecular weight (M_n and M_w) was determined using a Thermo Scientific Ultimate 3000 Gel Chromatography (GPC) instrument. The hydroxyl value was determined using an acetylation method. Viscosity was measured using a RV Brookefield viscometer. The Karl fisher titration method was employed to determine moisture content while volatile mater (VM, in %) was

measured using an IR heated balance. Finally, t-GAP was analysed for molecular weight, hydroxyl value (OH value), viscosity, density, VM and moisture content. The results are presented in Table 1.

Table 1. Physical and chemical properties of t-GAP

Properties	t-GAP
Colour	Brown
M_n	2000 ±100
OH value [mg KOH/g]	85 ±2
Viscosity [P]	17-20
Density [g/cm^3]	1.35
VM [%]	<0.1
Moisture [%]	<0.1

2.6 Reaction kinetics and concentration profiling data of t-GAP

For reaction monitoring, periodic sampling of the reaction mixture was done at distinct intervals from the time of attaining a reaction temperature of 90 °C and subjected to FTIR analysis without any prior treatment. A single bounce diamond ATR accessory has been employed for the subject study. Formation of t-GAP is indicated by a gradual growth of the peak at 2088 cm^{-1} attributed by $-N_3$ vibration of NaN_3, while consumption of t-PECH in the reaction is depicted by the disappearance of the peak at 747 cm^{-1} indicating a C–Cl bond. The area under the curves of the respective absorption peaks was considered to be proportional to the concentration of product and the reactants in the reaction. The spectroscopic data thus generated is plotted to create a concentration-time profiling of the reactant t-PECH as well as product t-GAP.

3 Results and Discussion

3.1 Spectroscopic study of t-GAP

Azidation of t-PECH with NaN_3 took place in DMSO as a solvent medium forming t-GAP. From Figure 4, it was observed that the peak corresponding to 747 cm^{-1} attributed to C–Cl bond vibration, disappeared after almost 5 h with no further advancement in the same. The same can also be verified with the progression of vibrational peak at 2088 cm^{-1}corresponding to that $-N_3$ bond as shown in Figure 5, representing formation of product t-GAP. However, to ensure completion of the azidation process, the reaction was continued for 6 h.

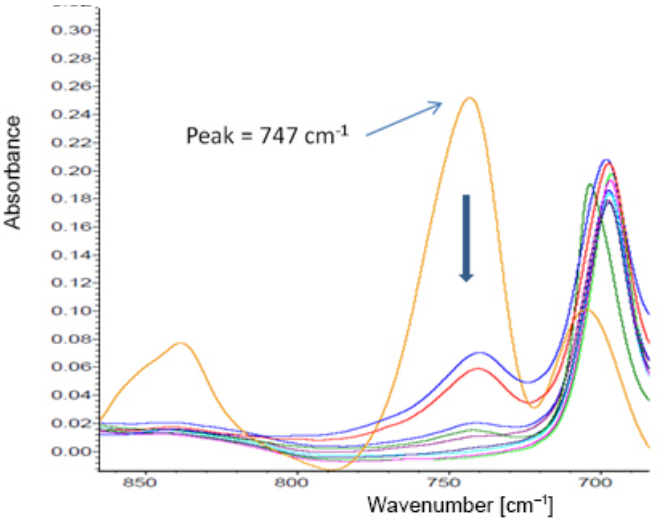

Figure 4. FTIR spectral regions corresponding to consumption of t-PECH

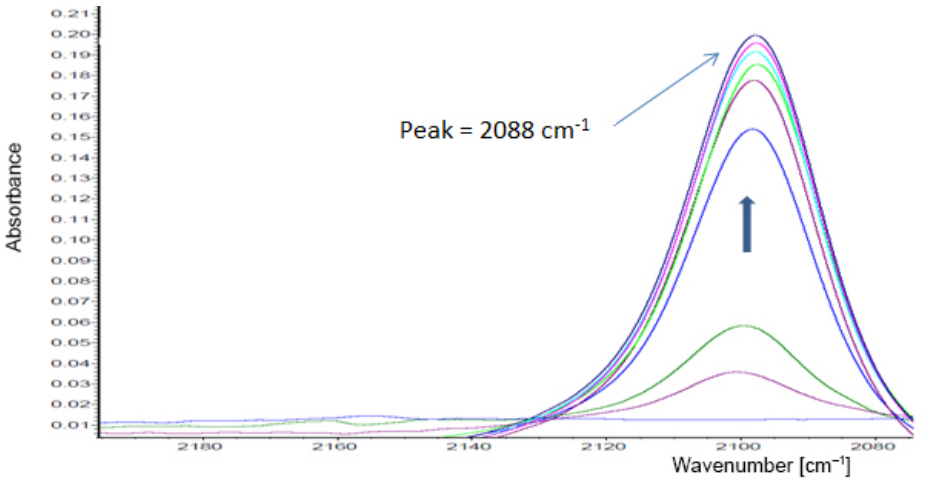

Figure 5. FTIR spectral regions corresponding to formation of t-GAP

3.2 Optimization of reaction

Lab level experiments were carried out at different reaction temperatures starting from 80 to 100 °C with the reaction mixtures being subjected to different time intervals of 20 to 4 h depending on the temperature. After completion of the process, the product, t-GAP was isolated and characterized using FTIR spectroscopy to assess if the reaction was completed or not. The absence of an

FTIR peak at 747 cm^{-1} corresponding to a C–Cl bond indicates that the reaction is complete. Table 2 depicts the completion of the reaction at different temperature/time intervals. During the laboratory scale experiments at temperatures of 95 and 100 °C, significant evaporation of DMSO solvent vapour was observed. Therefore, a reaction temperature of 90 °C was considered to be optimum with a reaction time of 6 h.

Table 2. Results of lab level process optimization batches

T_r [°C]	Time [h]	Presence of FTIR Peak at 747 cm^{-1} (corresponding to C–Cl bond)	Remarks
80	20	No	Complete
85	12	No	Complete
90	6	No	Complete
95	5	No	Complete
100	4	No	Complete

3.3 Rate kinetics and concentration profiling

FTIR data has been used to derive the relative concentration profile of both reactant and product. From the spectrums, the area under three peaks at distinct time intervals is taken to generate data of the concentration profile. Where, A_1 corresponds to area under the peak 747 cm^{-1}, A_2 corresponds to the area under the peak at 2088 cm^{-1} and A_3, corresponding to the area under the peakat 1040 cm^{-1} (–C–O–C– bond) which is common in both t-PECH and t-GAP. The ratio of A_1/A_3 and A_2/A_3 give effective relative areas under the peaks which can be considered as proportionate concentrations of t-PECH and t-GAP. These proportionate concentrations were then normalized to a scale of 100, as shown in Table 3.

The reaction shown in Figure 1 can be written as:

$$\alpha A + \beta B \rightarrow \varepsilon C + \mu D + \textit{other products}$$

where: A = t-PECH, B = azide ion, C= t-GAP and D = NaCl and C_A, C_B and so on are their corresponding concentrations.

The Rate of reaction expression can be written as:

$$-r_A = -\frac{dC_A}{dt} = -\frac{dC_B}{dt} = k\, C_A^{\,a} C_B^{\,b} .... \quad (1)$$

Table 3. Concentration of reactants and product derived from FTIR Spectroscopic data

t [min]	A_1 (under the peak 747 cm^{-1})	A_2 (under the peak 2088 cm^{-1})	A_3 (under the peak 1040 cm^{-1})	Relative conc. of t-PECH (C_A) ($=A_1/A_3$)	Relative conc. of t-GAP ($=A_2/A_3$)	Proportional conc. of t-PECH (C_A)	$1/C_A$
0	0.719	0	28.752	0.025006956	0	100	0.01
15	0.492	0.193	29.494	0.016681359	0.0065437	69.81404	0.014324
45	0.423	1.193	28.704	0.014736622	0.04156215	61.67502	0.016214
90	0.356	4.543	28.955	0.01229494	0.15689864	51.4562	0.019434
150	0.284	5.869	29.018	0.009787029	0.20225377	40.96021	0.024414
210	0.138	6.125	29.119	0.004739174	0.21034376	19.83417	0.050418
270	0.087	6.653	28.991	0.003000931	0.22948501	12.55936	0.079622
330	0.038	6.998	29.218	0.001300568	0.23950989	5.443076	0.18372
390	0.029	7.012	28.692	0.001010735	0.24438868	4.230079	0.236402

For constant stoichiometric ratio $C_B/C_A = \beta/\alpha$ =constant

$$-r_A = -\frac{dC_A}{dt} = \acute{K}\, C_A{}^n \tag{2}$$

where $n = a + b + ...$, $\acute{K}$ is the modified rate constant and n is the order of reaction.

To find out the reaction order, we first assume this reaction to be of 1st order. Therefore, Equation 2 after integration can be expressed as:

$$\text{Log}\,(C_{A0}/C_A) = \acute{K}\, t \tag{3}$$

Therefore, the graph between Log((C_{AO}/C_A)) and t should give a straight line. However, Figure 6 shows no such straight line. Hence the reaction cannot be first order.

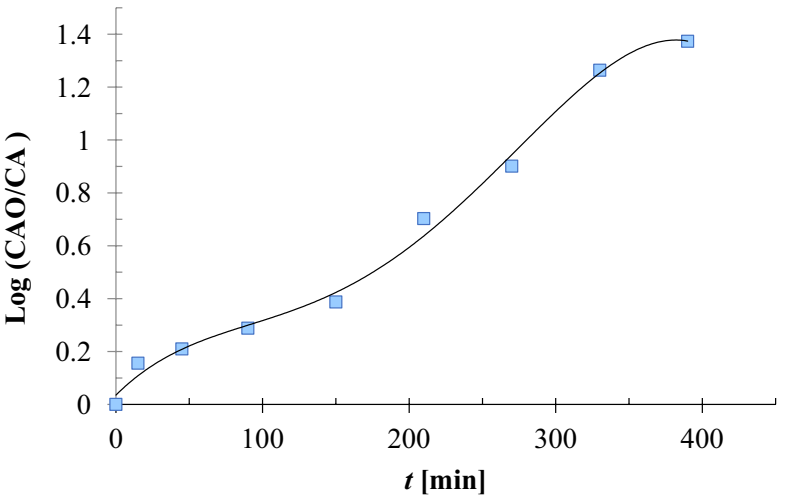

Figure 6. Concentration profile considered as 1st order kinetics

Now considering the reaction to be 2nd order. The same Equation 2 after integration can be written as:

$$\frac{1}{C_A} = \frac{1}{C_{A0}} + \acute{K}\, t \tag{4}$$

Thus, the graph between $1/C_A$ and t should give a straight line with slope $\acute{K}$ and intercept $1/C_{AO}$.

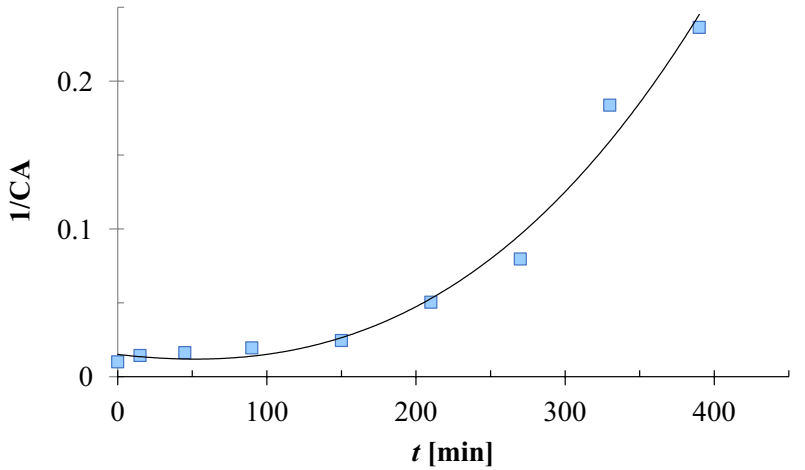

Figure 7. Concentration profile considered as 2nd order kinetics

From Figures 6 and 7, it is confirmed that the reaction does not obey 1st and 2nd order reaction kinetics.

After integrating Equation 2, for any n^{th} order reaction, for any fractional change in concentration of t-PECH, Equation 2 can be modified, according to [13], as:

$$C_A^{(1-n)} - C_{Ao}^{(1-n)} = \acute{K}\,(n-1)\,t \tag{5}$$

$$t_F = \frac{F^{1-n}-1}{\acute{K}(n-1)}\; C_{Ao}^{(1-n)} \tag{6}$$

where:

Logarithms of Equation 6 will give:

$$\text{Log } t_F = \log\left(\frac{F^{(1-n)}-1}{\acute{K}(n-1)}\right) + (1-n)\log C_{Ao} \tag{7}$$

For illustration, considering $F = 0.80$, Equation 7 can be written as:

$$\text{Log } t_F = \log\left(\frac{0.8^{(1-n)}-1}{\acute{K}(n-1)}\right) + (1-n)\log C_{Ao} \tag{8}$$

where t_F is the time needed for fractional change (80%) in concentration. After

taking any three values of C_A and C_{AO} at any distinct time on the graph between C_A and t, the following calculation can be carried out for 80% fractional change.

Table 4. Logarithmic fractional concentration and t for nth order reaction

C_{A0}	$C_A = 0.80C_{AO}$	t_F (from graph)	Log t_F	Log C_{AO}
100	80	20	2	1.30103
60	48	25	1.778151	1.39794001
20	16	44	1.30103	1.64345268

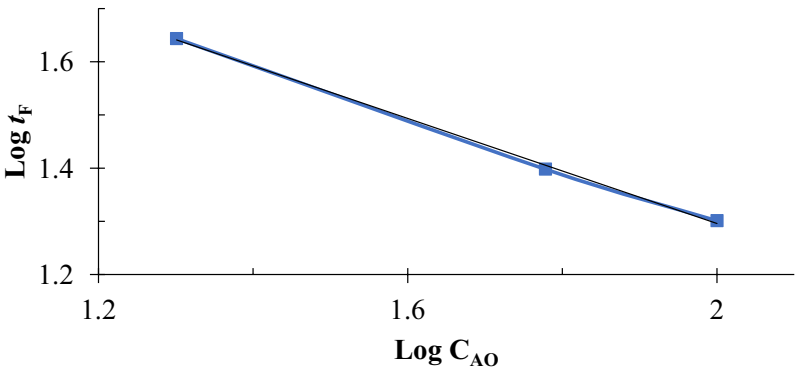

Figure 8. Logarithmic fractional concentration and t for nth order reaction

Figure 8 gives almost a straight line with a slope value of –0.493 and intercept of 2.283. Now, from Equation 8, the value of n and $\acute{K}$ can be calculated as:

$(1 - n) = -0.493 \Rightarrow n = 1.493$

$\log\left(\frac{0.8^{(1-n)}-1}{\acute{K}(n-1)}\right) = 2.283 \Rightarrow$ After putting the value of $n = 1.493$, the value of $\acute{K} = 1.23\times10^{-3}$.

Finally the overall rate of reaction can be represented as:

$$-r_A = 1.23 \times 10^{-3}\, C_A^{1.493} \quad (9)$$

Equation 9 represents the rate equation for the preparation of t-GAP from the precursor t-PECH. The rate equation can predict the progress of reaction at any point of time during the process and time required for completion of the reaction at the given temperature.

4 Conclusions

- In the study, FTIR spectroscopy has been used as an effective tool for determining the time required for completion of reaction for preparation t-GAP at different temperatures and accordingly, the reaction conditions have been optimized.
- The azidation process of t-PECH to t-GAP has been further systematically studied using FTIR spectroscopy and the data on concentration profile of both reactant and product have been generated for the progress of reaction. The periodic probing with FTIR spectroscopy suggested the t-GAP reaction to be completed within 6 h while reaction temperature is maintained at 90 °C. It is also observed that, initially, the conversion rate is quite high but after 4.5-5 h it became very slow.
- The effective area under the peak method was employed to calculate the concentration profile of t-GAP and t-PECH, the same being used to derive the reaction kinetic parameters. The FTIR spectroscopic study on rate kinetics, could successfully generate kinetic parameters like reaction order n as 1.493, and rate constant $= 1.23 \times 10^{-3}$ at 90 °C. The reaction kinetics data can be advantageously used to predict the progress of the reaction at any point of time during the process of preparation of t-GAP and time required for completion of the reaction.
- The finding confirms that FTIR spectroscopy can be used as an efficient tool to generate relative concentration profiles of reactants/products; and the same can be used to derive reaction kinetic parameters and rate equation.

Acknowledgement

The authors of this manuscript are very grateful to the Director, HEMRL for his valuable support and for giving us the opportunity to carry out this work.

References

[1] Provatas, A. *Energetic Polymers and Plastics for Explosive Formulations — A Review of Recent Advances.* DSTO-TR-0966, Commonwealth of Australia, Canberra, **2000**.

[2] Agrawal, J.P.; Hodgson, R. *Organic Chemistry of Explosives.* John Wiley & Sons Ltd, Chichester, **2007**; ISBN-13 978-0-470-02967-1.

[3] Kubota, N. Propellants and Explosives, Thermochemical Aspects of Combustion. 2nd Ed., Wiley-VCH Verlag GmbH & Co. KG, Weinheim, Germany, **2007**; ISBN 978-3-527-31424-9.

[4] Agrawal, J.P. *High Energy Materials, Propellants Explosives and Pyrotechnics.* Wiley-VCH Verlag GmbH & Co. KG, Weinheim, Germany, **2010**; ISBN 978-3-527-32610-5.
[5] Frankel, M.B.; Grant, L.R.; Flanagan, J.E. Historical Development of Glycidyl Azide Polymer. *J. Propul. Power* **1992**, *8*: 550-563; https://doi.org/10.2514/3.23514.
[6] Nazare, A.N.; Asthana, S.N.; Singh, H. Glycidyl Azide Polymer (GAP) – An Energetic Component of Advanced Solid Rocket Propellants – A Review. *J. Energ. Mat.* **1992**, *10*(1): 43-63; https://doi.org/10.1080/07370659208018634.
[7] Nguyen, C.; Morin, F.; Hiernard, F.; Guengant, Y. High Performance Aluminized GAP-based Propellants – IM Results. *Proc. Insensitive Munitions & Energetic Materials Technology Symp.,* Munich, Germany, **2010**.
[8] Da Silva, G.; Rufino, S.C.; Iha, K. Green Propellants: Oxidizer. *J. Aerospace Technol. Manage.* **2013**, 5.2.
[9] Wingborg, N.; Andreasson, S.; de Flon, J.; Johnsson, M.; Liljedahl, M.; Oscarsson, C.; Petterssons, Å.; Wanhatalo, M. Development of ADN-based Minimum Smoke Propellants. Proc. *46th AIAA/ASME/SAE/ASEE Joint Propulsion Conference & Exhibit,* **2010**, paper 2010-6586, Nashvile, https://doi.org/10.2514/6.2010-6586.
[10] Gettwert, V.; Franzin, A.; Bohn, M.A.; DeLuca, L.T.; Heintz, T.; Weiser, V. ADN/GAP Composite Propellants with and without Metallic Fuels. *Proc. 10th Int. Symp. Special Topics in Chemical Propulsion & Energetic Materials* (10-ISICP), Poitiers, France, **2014**.
[11] DeLuca, L.T.; Palmucci, I.; Franzin, A.; Weiser, V.; Gettwert, V.; Wingborg, N.; Sjöblomc, M. New Energetic Ingredients for Solid Rocket Propulsion. *Proc. 9th Int. High Energy Materials Conf. and Exhibit* (HEMCE), Thiruvananthapuram, Kerala, India, **2014**.
[12] Gettwert, V.; Fischer, S.; Menke, K. Aluminized ADN/GAP Propellants – Formulation and Properties. *Proc. 44th Int. Annu. Conf. Fraunhofer ICT*, Karlsruhe, Germany, **2013**, P57.
[13] Menke, K.; Heintz, T.; Schweikert, W.; Keicher, T.; Krause, H. Formulation and Properties of ADN/GAP Propellants. *Propellants Explos. Pyrotech.* **2009**, *34*: 218-230; https://doi.org/10.1002/prep.200900013.
[14] Klapotke, T.M.; Suceska, M. Theoretical Evaluation of TKX-50 as an Ingredient in Rocket Propellants. *Z. Anorg. Allg. Chem.* **2021**, *647*: 572-574; https://doi.org/10.1002/zaac.202100053.
[15] Hussein, A.K.; Elbeih, A.; Zeman, S. The Effect of Glycidylazide Polymer on the Stability and Explosive Properties of Different Interesting Nitramines. *RSC Adv.* **2018**, *8*: 17272-17278; https://doi.org/10.1039/C8RA02994F.
[16] Ampleman, G. *Glycidyl Azide Polymer.* US Patent 5,359,012, **1994**.
[17] Soman, R.R.; Athar, J.; Agawane, N.T.; Shee, S.; Gore, G.M.; Sikder, A.K. Synthesis, Characterization and Rheology of Tetrafunctionalglycidylazide Polymer vis-a`-vis Difunctional GAP. *Polym. Bull.* **2016**, *73*: 449-461.
[18] Pintar, A.; Batista, J.; Levec, J. *In Situ* Fourier Transform Infrared Spectroscopy as an Efficient Tool for Determination of Reaction Kinetics. *Analyst* **2002**, *127*(11):

1535-1540; https://doi.org/10.1039/B207204A.
[19] Ye, S.; Yang, S.; Ni, L.; Qiu, W.; Xu, Q. Mechanism and Kinetic Study of Paal-Knorr Reaction Based on *In-Situ* MIR Monitoring. *Spectrochim. Acta A* **2022**, *264*: paper 120280; https://doi.org/10.1016/j.saa.2021.120280.
[20] Levenspiel, O. Interpretation of Batch Reactor Data. In: *Chemical Reaction Engineering.* 3rd Ed., John Wiley & Sons, **1999**, pp. 38-75; ISBN 978-0471254249.

Received: October 15, 2023
Revised: June 24, 2024
First published online: June 28, 2024